Electrocatalytic oxidation of H₂S by a ZrO₂ catalyst on biochar carbon

N. Shukova^{1*}, D. Uzun², E. Razkazova-Velkova¹, K. Petrov² A. Gigova², O. Dimitrov², M. Dimitrova², L. Ljutzkanov¹

¹Institute of Chemical Engineering, Bulgarian Academy of Sciences, Acad. G. Bonchev Str., Bl. 103, Sofia 1113, Bulgaria

²Institute of Electrochemistry and Energy Systems "Acad. Evgeni Budevski", Bulgarian Academy of Sciences, Acad. G. Bonchev Str., Bl. 10, Sofia 1113, Bulgaria

Received: April 01, 2025; Revised: July 31, 2025

A catalyst based on ZrO₂ incorporated into a biochar carbon matrix was synthesized. The biochar was obtained from pyrolyzed sunflower husks. The ZrO₂ deposit onto carbon sunflower husks (ZCSH) was intended for usage in the electrooxidation of sulfide ions from a model solution containing 65 mg/l of S²- and 18 g/l of NaCl. The electrocatalyst was characterized by scanning electron microscopy, X-ray diffraction and BET. Electrodes were manufactured with different amounts of catalyst (20 to 80 mg/cm²), binder (Teflon®) and Vulcan® XC-72. Their electrochemical properties were studied by means of cyclic voltammetry, galvanostatic measurements and Tafel slopes. The electrodes with 40 mg/cm² of catalytic mass within the electrode exhibited a lower overvoltage following the galvanostatic measurements.

Keywords: Hydrogen sulfide, ZrO2 catalyst, Fuel cells, Electrodes

INTRODUCTION

The origin of sulfides can be generally divided into natural and anthropogenic. Natural sources include volcanoes, hot springs, and closed deep-sea basins (where sulfides are formed from sulfurcontaining organic matter by sulfate-reducing bacteria). The main anthropogenic pollution with sulfides stems from the petroleum, leather, pulp and textile industries, sewage systems and wastewater treatment plants [1, 2]. The conventional methods for treatment of such effluents are sorption methods, that can be combined with oxidation with strong oxidants [3-7], precipitation with metals [8] or biological oxidation [9-11]. Thermal and electrical methods for decomposition are also developed [12, 13]. The Claus process is a classical method but it requires high temperatures and specific catalysts [14]. There are many catalysts and photocatalysts that convert H₂S in gaseous [10, 15–16] or dissolved form of sulfur. It is reported that Me²⁺ cations (Me=Mn, Co, Ni, Fe, Cu) catalyze the process of oxidation of H₂S [17, 18]. In many cases the main product is elemental sulfur that is undesirable both of environmental point of view and because it inhibits the oxidation by blocking the active sites of the catalyst. The processes that involve adsorption on different adsorbents in many cases use waste organic products for deriving adsorbents. This is a promising trend for the circular economics [19, 20] by converting wastes to valuable products. Biochar,

produced from agricultural wastes or sludge [21–24] limited-oxygen conditions, is rapidly emerging as an environmental restoration material. It is cheap, of large surface area, low cost, low energy consumption, high cation-exchange capacity, and stable structure [25]; it is a promising substitute for traditional anode catalysts which are expensive and environmentally harmful [26]. The biochar has high oxidation reduction reaction (ORR) catalytic activities. The latter is very important for the efficiency of fuel cells and metal-air batteries. It should be noted that biochar, as an electrocatalyst for microbial fuel cells (MFC), is a relatively new field, therefore, there is a wide scope for further investigations and applications [27]. Fuel cells (FC) and microbial fuel cells (MFC) are a promising new approach for decontamination of pollutants with simultaneous electricity generation [28, 29]. In our previous investigations, a catalyst for sulfide oxidation based on active carbon and ZrO₂ incorporated in a matrix of biochar, is reported [30, 31]. These studies are focused on the catalyst use for hydrogen sulfide wastewater treatment. In order to use a catalyst in fuel cells it is necessary to study its electrocatalytic properties and to design electrodes with suitable electrochemical characteristics.

The aim of the present study is to manufacture electrodes based on ZrO_2 over a biochar from sunflower husks, suitable for use in a FC.

^{*} To whom all correspondence should be sent: E-mail: nastemi1@abv.bg

MATERIALS AND METHODS

Catalyst preparation and characterization

The preparation method of the catalyst is a patented technology [32] that includes impregnation of the organic material (sunflower husks) with ZrCl₄ (Merck, ≥99.5% on trace metals basis) as a precursor salt and subsequent pyrolysis with simultaneous activation with water vapor and the flue gases from the pyrolysis. The process was conducted at 680 °C with a heating rate of 13°C per min and holding for 45 min at the final temperature. The obtained catalyst is ZrO₂ incorporated into the activated carbon matrix at a ratio of 1:3. The ZrO₂ incorporated into the biochar carbon matrix (ZCSH) was characterized by Brunauer-Emmett-Teller analysis (BET), X-ray diffraction analysis (XRD), and scanning electron microscopy analysis (SEM). XRD patterns were recorded on a Philips diffractometer using CuK radiation (λ =1.54178 Å, 40 kV and 30 mA) with a scanning rate of 2 min⁻¹. The scan range size was $10-100^{\circ}2\theta$ with 0.04° step size and 2s per step. The crystallite sizes (t) were determined by Scherer's formula: $t = \kappa \lambda / B\cos\theta$. where k is shape factor (k = 0.9 for spherical crystals with cubic symmetry), λ (Å) is the wavelength, θ is the diffraction angle of the peak, B (rad) is the line broadening at the FWHM (full width at half maximum) values of the peaks. BET studies were carried out on a Quantachrome Autosorb iQ (USA) instrument that measures the quantity of gas adsorbed onto or desorbed from a solid surface at an equilibrium vapor pressure by the static volumetric method.

The analytical procedures were applied in order to determine the morphology, surface area, pore diameter and distribution, etc. All the properties are important for characterization of a catalyst.

Electrode manufacturing

The electrodes were manufactured with Vulcan $^{\$}$ XC72 (conductive carbon black, particle size ~ 50 nm, Merck) and Teflon $^{\$}$ (PTFE powder, freeflowing, 1 μ m particle size, Merck) as a binder. All electrodes had a geometric area of 1 cm² and were prepared from a mixture of catalyst, Teflon (35%) and Vulcan XC72 (60 mg/cm²). Different electrodes with 20 mg, 40 mg, 60 mg, 80 mg of ZrO₂ catalyst and without a catalyst were obtained. The mixture (catalyst, Teflon and Vulcan XC72) was pressed on both sides of a current collector, which is a stainless-steel mesh (1 cm²) at 300 $^{\circ}$ C and a pressure of 300 atm.

Experimental equipment, conditions and electrochemical analysis

The electrolyte solution contained sodium sulfide (Na₂S.9H₂O, ACS reagent, \geq 98.0%, Merck) and sodium chloride (NaCl, Merck). The concentration of S²⁻ in the electrolyte was 65 mg/l and that of NaCl - 18 g/l. These concentrations were chosen from our previous investigation [30] as those providing the most appropriate rate of oxidation. NaCl was added in order to improve the conductivity of the solution (this is the salinity of the Black Sea) [30]. The hydrogen sulfide from Black Sea can be utilized in fuel cells.

The 1 cm² electrodes were studied by cyclic voltammetry, steady-state polarization curves and Tafel analysis. The cyclic voltammetry measurements were done on a Solartron 1286 electrochemical The analyzer. polarization characteristics were determined on a Tacussell bipotentiostat type BI-PAD. Minimum three measurements were made for each result to achieve better reproducibility. Arithmetic averages are presented in the graphs. Galvanostatic measurements were made with Solartron 1286 (Fig. 1) at room temperature and a cell volume of 50 ml. The reference electrode was a reversible hydrogen electrode (RHE) (Gaskatel). The counter-electrode was platinum foil.

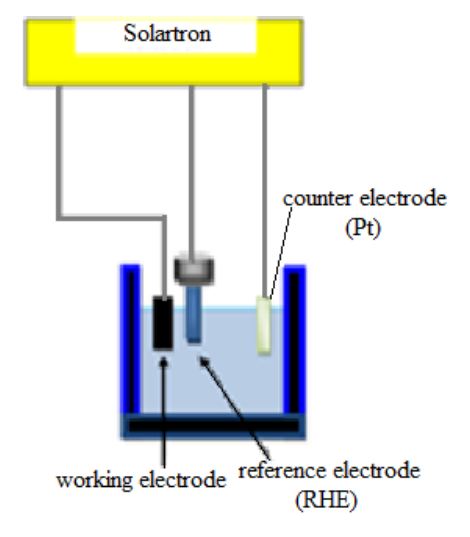


Fig. 1. Scheme of the three-electrode cell

RESULTS AND DISCUSSION

XRD studies

The samples were examined using a Philips X-ray diffractometer PW 1030.

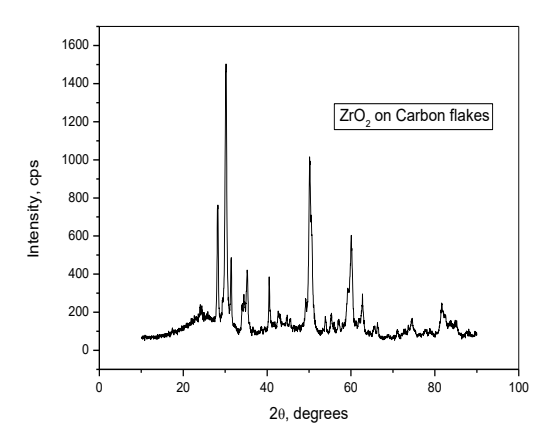
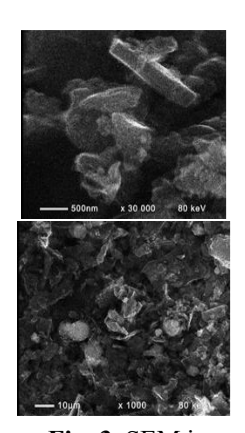


Fig. 2. XRD of the ZrO₂ on sunflower husks

In the literature peaks are observed at 2 theta for tetragonal and monoclinic zirconia, respectively [33]. In our studies XRD peaks, as presented in Fig. 2, are manifested at 24°, 28°, 30°, 35°, 40°, 50°, 60°, 63°, corresponding to the diffraction patterns of (111), (200), (220), (311), (222) and (400), likewise clearly tetragonal and monoclinic zirconia are present, matching the hexagonal wurtzite single crystal structure with the standard ZrO₂ (PDF card #82e1245).

SEM studies



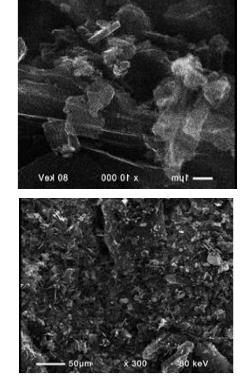


Fig. 3. SEM images of ZrO₂ on sunflower husks

Scanning electron microscopy (SEM) images of the ZrO₂ surface morphology, obtained at different magnifications, are shown in Figure 3. The morphology of the pure ZrO₂ includes rectangular shapes of 20×500 nm. The material has an irregular network structure with a variety of large and small round particles, a rigorous structure with voids interacting with the solution, together with a hierarchy of channels aiding the processes of molecular diffusion leading to the catalytic reactions observed.

BET studies (surface area and pore size analysis)

Isotherms of the type shown in Figure 4 reveal that the adsorbate-adsorbent interactions are relatively weak. The steep vertical rise of the isotherms near P/Po = 1 indicates the presence of macropores in the measured samples.

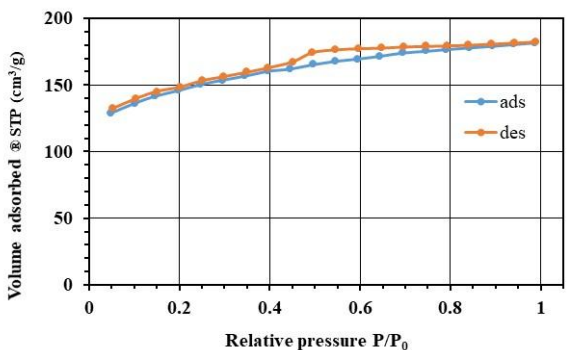


Fig. 4. BET isotherms of the ZrO₂ on sunflower husks

The specific surface area was determined by the BET method. Multipoint BET was determined at a relative pressure in the range p/p0 = 0.1-0.3; and single-point BET at p/p0 = 0.3. The pore volume was read at a relative measurement pressure close to 1 (p/p0 = 0.99). The pore diameter was calculated assuming that the pores have a cylindrical geometry, at p/p0 = 0.99. The results are summarized in Table 1

Table 1. BET structural characteristics of ZrO₂

Characteristics	Pure husk	ZrO ₂ onto biochar
Surface area (multi-point BET), m²/g	477	430
Surface area (single-point BET), m ² /g	497	445
Total pore volume, cm ³ /g	0.301 for pores < 142 nm (D)	0.268 for pores < 160 nm (D)
Average pore diameter, (4V/S), nm	2.5	2.5

The presence of macro and mesopores facilitates the catalytical process, the adsorption of the reagents and the desorption of the products.

Polarization curve analysis

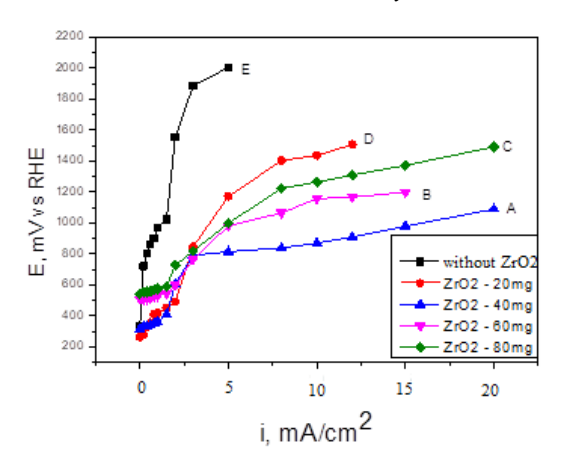


Fig. 5. Galvanostatic polarization curves of the electrodes as a function of the amount of ZrO₂ catalyst.

Figure 5 shows the polarization curves of the electrodes obtained for 20 mg, 40 mg, 60 mg, 80 mg of ZrO₂ catalyst, and without a catalyst. The figure shows that electrode (A) containing 40 mg of ZrO₂ catalyst and 60 mg of Vulcan XC-72 has the best electrochemical characteristics providing the lowest overpotential. The electrode containing 60 mg of ZrO₂ catalyst and 60 mg of Vulcan XC-72 provides a slightly higher overpotential and, hence, has inferior characteristics.

Tafel analysis

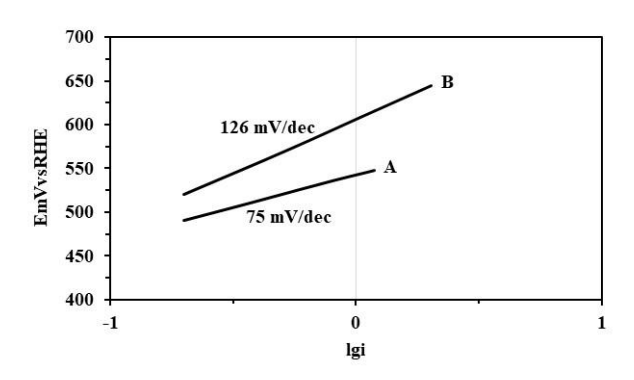


Fig. 6. Tafel slopes of electrodes containing 40 mg (A) and 60 mg (B) of ZrO_2 catalyst.

The Tafel slopes presented in Fig. 6 are of the two electrodes (A and B), with the best electrochemical characteristics given in the polarization curves shown in Fig. 5. The figure (Figure 6) shows that electrode A, containing 40 mg of ZrO₂ catalyst and 60 mg of Vulcan XC-72, possesses the best kinetic parameters. The results of Tafel slopes of 75 mV and 126 mV/dec, respectively, are close to literature data [34] for ZrO₂ catalyst. This improves the understanding of the electrocatalytic mechanisms of ZrO₂ catalyst supported on sunflower husks, but also

paves the way for its application in efficient and sustainable energy systems.

Cyclic voltammetry studies

It is observed that there are a pair of redox peaks for the electrode with 40 mg/cm². They can be found at 108, 90, 101 and 95 mV (Figure 7). The multiple peaks indicate the presence of electrochemical activity of the electrode in the selected solution. The availability of many peaks demonstrates the occurrence of different chemical reactions. This is to be expected, given the possibility of occurring of multiple chemical transformations of sulfur ions.

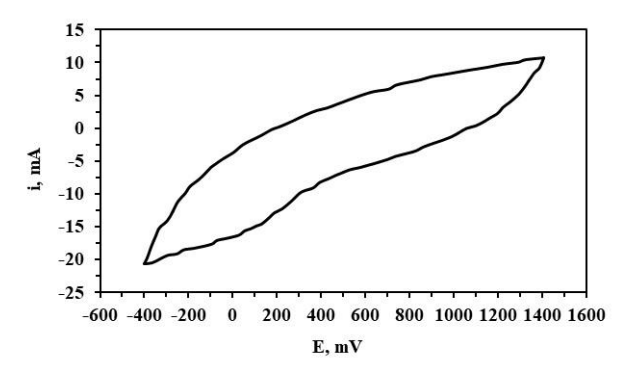


Fig. 7. Cyclic voltammogram *of* a ZrO_2 electrode, electrolyte (65 mg/l S^{2-} +18 g/l NaCl); $T = 25^{\circ}C$

CONCLUSIONS

ZrO₂ catalyst was synthesized on sunflower husks. It was characterized by XRD that showed tetragonal and monoclinic zirconia and hexagonal wurtzite single crystal structure of standard ZrO₂. The BET isotherms showed that the adsorbate-adsorbent interactions are relatively weak. The morphology of the pure ZrO₂ includes rectangular shapes of 20×500 nm. The material possesses an irregular network structure with a variety of large and small round particles.

At low current densities (up to 5 mA / cm²) the measured electrodes show similar characteristics. At high current densities, the electrode containing 40 mg of ZrO₂ catalyst and 60 mg of Vulcan XC-72 shows the best electrochemical characteristics.

Acknowledgement: This research was funded by the Bulgarian National Science Fund, Grant No KP-06-N67/6 from 12 December 2022.

REFERENCES

- W. H. Smith, Encyclopedia of Biodiversity, 2nd edn., Explore book, 2001.
- 2. S. L. M. Rubright, L. L. Pearce, J. Peterson, *Environ. Toxicol. of hydrogen sulfide*, **71**, 1-13 (2017).
- 3. R. Cotrino, A.D. Levine, P. Amitzoglou, J. S. Perone, *Florida Water Res. J.*, (A-72), 22-25 (2007).
- M. Seredych, T. J. Bandosz, Chem. Eng. J., 128 (1), 59-68 (2007).
- 5. R. Wang, Sep. Purif. Technol., 31, 83-89 (2003).
- S. Yasyerli, I. Ar, G. Dogu, T. Dogu, *Chem. Eng. Process.*, 41 (9), 785-792 (2002).
- M. Tomar, T. H. A. Abdullah, Water Res., 28, 2545-2552 (1994).
- 8. M. Henze, P. Harremoës, J. la Cour Jansen, E. Arvin, Wastewater Treatment: Biological and Chemical Processes, 2nd edn., Springer, Berlin, 1997.
- T. Jia, L. Zhang, X. Li, Q. Zhao, Y. Peng, J. Sui, Ch. Wang, Sci. Total Environ., 857(Part 3), 1-20 (2023).
- 10. O. I. Dada, L. Yu, Sh. Neibergs, Sh. Chen, *Renew. Sustain. Energy Rev.*, **209**, 1-13 (2025).
- 11. G. Xia, Zh. Sun, J. Huang, J. Qi, J. Yao, *J. Environ. Manag.*, **367**, 1-20 2024.
- 12. G. Özgül, A. S. Koparal, Ü. B. Öğütveren, *Sep. Purif. Technol.*, **62**, 656 (2008).
- 13. J. Zaman, A. Chakma, Fuel Process. Technol., 41, 159-198 (1995).
- M. Capone, J. K. Kroschwitz, M. HoweGrant, Encyclopedia of Chemical Technology, 23, Wiley, New York, 1997.
- 15. Y. Xu, Zh. Ma, Zh. Wang, Ch. Liu, Y. Yang, *J. Ind. Eng. Chem.*, **136**, 524-531 (2024).
- Y. Yu, T. Zhang, L. Zheng, J. Yu, Chem. Eng. J., 225, 9-15 (2013).
- U.S. National Research Council, Hydrogen sulfide. Committee on Medical and Biologic Effects of Environmental Pollutants, 38 Subcommittee on Hydrogen Sulfide. University Park Press, Baltimore, MD, 1979.
- P. K. Dutta, K. Rabaey, Zh. Yuan, J. Keller, Water Res., 42, 317-322 (2008).

- T. Yuan, K. Hashimoto, A. Tazaki, M. Hasegawa, F. Kurniasari, Ch. Ohta, M. Aoki, N. Ohgami, M. Kato, J. Environ. Manage. 321 1-8 (2022).
- 20. D. Ouyang, Y. Chen, J. Yan, L. Qian, L. Han, M. Chen, *Chem. Eng. J.*, **370**, 614-624 (2019).
- S. Marzorati, A. Goglio, S. Fest-Santini, D. Mombelli, F. Villa, P. Cristiani, A. Schievano, *Int. J. Hydrogen Energy*, 44, 4496-4507 (2019).
- 22. J. Huang, H. Feng, Y. Jia, D. Shen, Y. Xu, *Water Sci. Technol.*, **80**, 1-17 (2019).
- 23. H.-C. Chang, W. Gustave, Z.-F. Yuan, Y. Xiao, Z. Chen, *Environ. Technol. Innov.*, **18**, 1043-1070 (2020).
- 24. X. Gong, L. Peng, X. Wang, L. Wu, Y. Liu, *Int. J. Hydrogen Energy*, **45**, 15336-15345 (2020).
- 25. Q. Hang, H. Wang, Z. Chu, B. Ye, Ch. Li, Z. Hou, *Environ. Sci. Pollut. Res.*, **23**, 8260 8274, (2016).
- 26. J. Lee, K.-H. Kim, E.E. Kwon, *Renew. Sustain. Energy Rev.*, 77, 70-79 (2017).
- 27. Sh. Li, Sh.-H. Ho, T. Hua, Q. Zhou, F. Li, J. Tang, *Green Energy & Environ.*, **6**, 1-16 2021, https://doi.org/10.1016/j.gee.2020.11.010.
- 28. L. Zhong, Sh. Zhang, Y. Wei, R. Bao, *Biochem. Eng. J.*, **124 (6)**, 6-12 (2017).
- 29. K. Wang, Sh. Zhang, Zh. Chen, R. Bao, *Chem. Eng. J.*, **341**, 184-190 (2018).
- 30. N. Dermendzhieva, E. Razkazova-Velkova, M. Martinov, L. Ljutzkanov, V. Beschkov, *J. Chem. Technol. Metall.*, **48** (5), 465-468 (2013).
- N. Dermendzhieva, E. Razkazova-Velkova, V. Beschkov, *Bulg. Chem. Commun.*, **52**, 35-38 (2020), ISSN: 0861-9808, DOI:10.34049/bcc.52.A.317.
- 32. L. Ljutzkanov, A. Atanasov, BG patent № 63594 /26.06.2002.
- 33. J. Chevalier, L. Gremillard, A.V. Virkar, D. R. Clarke, *J. Am. Ceram. Soc.*, **92** (9), 1901-1920 (2009), https://doi.org/10.1111/j.1551-2916.2009.03278.x
- 34. A. G. Rojek, Gr. Leniec, E. Mijowska, *Appl. Surf. Sci.* **684** (161851) 1-8 (2025).